

BAND GAP STRUCTURES OF PBG AND ROD-LOADED CAVITIES*

A. V. Smirnov, R. Yi, D. Yu, DULY Research Inc., Rancho Palos Verdes, CA 90275, U.S.A.

Abstract

Cavities loaded by a lattice with many rods, or just a few rods are considered for single-beam, flat-beam and multi-beam applications. Lossy periphery effect on Q-factor was simulated with both 3D and 2D codes. The Photonic Band Gap (PBG) effect is demonstrated as a Q-factor reduction by 2-3 orders for *all* HOMs of a single-defect cavity. The “PBG effect” signature is found even for cavities loaded with a single circle of rods (first-order lattice). Six-beam and two-sheet-beam topologies demonstrate effective reshaping of the fields of the operating mode but do not possess the unique Q-factor discrimination found for a single-beam cavity.

INTRODUCTION

Photonic (or Electromagnetic) Band Gap (PBG/EBG) and frequency-selective structures (or surfaces, FSS) are used nowadays in various microwave and wireless devices as effective filters, antennas, sensors, and composite materials. In an unbounded lattice, a 3D PBG structure can have common features with left-handed media [1] as well. A notable paper by N. Kroll *et al.* [2] has attracted growing interest of researchers in the area of new pulsed power generating and accelerating PBG structures. We characterize here the “PBG effect” in practical terms of Q-factor modal selectivity. We demonstrate that rod-loaded structures can be effectively applied for multi-beam topologies using both circular and flat beams.

SINGLE-DEFECT PBG CAVITY

We recalculated the PBG effect in a 2D single-defect triangular lattice more accurately with both 3D GdfidL (Gd1 [3]) and 2D SUPERFISH [4] eigenmode solvers. Similar to our previous paper [5] we characterize the PBG effect in a convenient way by the ratio of the Q-factor in the presence of highly-resistive or absorbing periphery, to the Q-factor for all-copper boundaries. A reason of the recalculation is an unphysical dip in the curves for the fundamental mode Q-factor [5,6] obtained with an older version code [7]. The corrected ratios for an X-band, 36-rod PBG cavity are plotted as a function of the ratio of the rod radius a , and the space period b in Figure 1 for perfect absorbing boundary. Since the fundamental frequency f_{01} depends on a/b , in the 3D cavity model the longitudinal gap is scaled as $7.87mmf_{XB}/f_{01}$, and the absorber radial thickness scaled as $a(2+f_{XB}/f_{01})$, where $f_{XB}=11.4GHz$. For resistive wall periphery ($\sigma_w=0.6\text{ Sm/m}$), the plots (not shown) are essentially the same as Figure 1, but the Q-factor drop for the dipole mode is a little bit less rapid near the bifurcation point $a/b=0.21$.

* Work supported by DOE SBIR grant no. DE-FG02-03ER83845

As it can be seen from Figure 1 the “good” region for damped dipole mode operation is $0.14 < a/b < 0.21$ which is wider than we found earlier [5, 6]. Nearly perfect damping of as many as a hundred TM_{MN0} HOMs can be seen in Figure 2 where ratios of the HOM Q-factors to the fundamental Q-factor are given in the middle of the “good” region in a log scale. One can see that matched absorber gives about one order better damping for the lowest HOMs than resistive periphery.

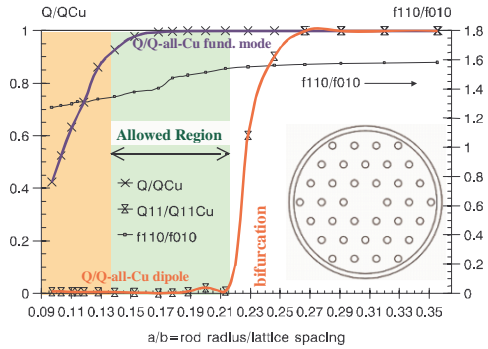


Figure 1: Q-factor reduction with respect to all-copper cavity for TM_{010} and TM_{110} modes in a 36-rod cavity having idealized periphery absorber with $\epsilon=0.8+0.6i=\mu$.

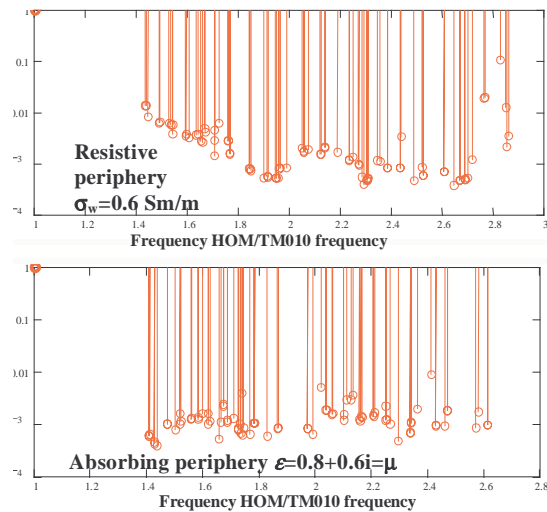


Figure 2: Q-factor for HOMs related to fundamental mode Q-factor vs. HOM frequency normalized by fundamental frequency at $a/b=0.168$. No transverse symmetry applied.

The calculations show that compared with absorbing periphery, damping of HOMs is less perfect with resistive metal periphery within the allowed region. There is another feature distinguishing lossy metal from matched absorber: presence of asymmetric HOMs with substantial (compared to fundamental mode) Q-factor. This feature is illustrated in Figure 3 in a linear scale for $a/b=0.15$ and 0.13 . Practically it means that a real $|\epsilon|>1$, $|\mu|>1$ absorber might need to be shaped as a 2D anechoic chamber [8].

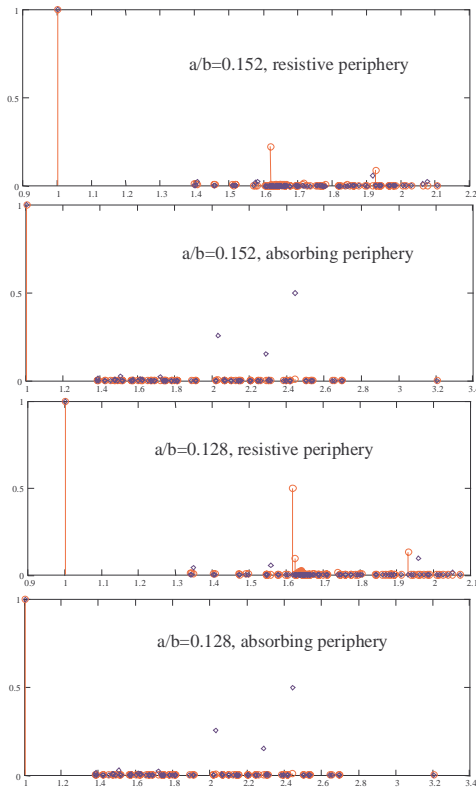


Figure 3: The same as in Figure 2, but for other values of a/b from the “allowed” region, and, additionally, the diamonds represent corresponding r/Q ratios.

To check the Q-factor calculations, we also used the SUPERFISH code for 2D modeling. A postprocessor was written to handle properly the complementary boundary conditions. The results of Q-factor damping are given in Figures 4 and 5 for an idealized periphery absorber with $\epsilon=0.8+0.6i=\mu$. Taking into account end wall losses are not included in SUPERFISH calculations, the agreement between 2D and 3D results for the same (resistive or absorbing) periphery is considered very good.

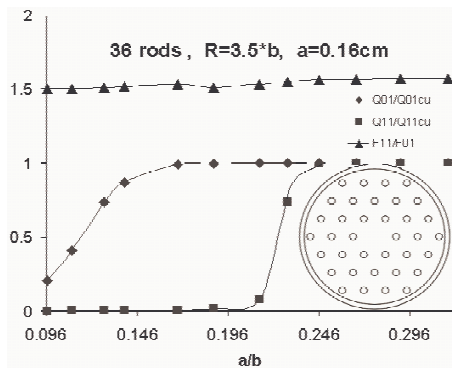


Figure 4: Complementary boundary SUPERFISH results: Q-factor ratio of damped cavity with respect to all-copper (non-damped) cavity for fundamental and dipole mode.

A damped cavity with just a single circle of 12 rods possesses similar features of selective Q-factor suppression. Although there are no abrupt Q-bifurcation as the 36-rod cavity, we still can have 15 times lower Q for dipole mode, and a factor of 4 suppression of the

second monopole mode whereas the fundamental mode is degraded only by 15% at $a/b=0.12$ (see Figure 5).

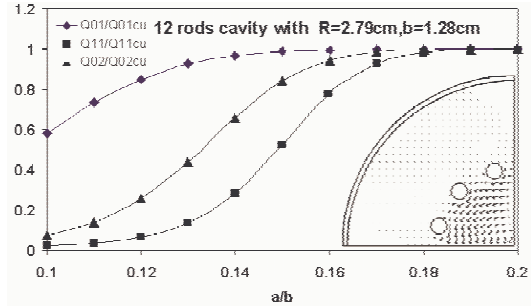


Figure 5: Complementary boundary SUPERFISH results: Q-factor with idealized periphery absorber related to all-copper cavity for fundamental, dipole and TM_{020} modes for only one circle of 12 rods. (Inset shows one-quarter model).

6-BEAM CAVITY AND CENTRAL COUPLING

We continue here a 6-beam cavity study with enlarged distance between beams (2.5-3cm vs. 1.1cm of the first design [6]) to accommodate better beam optics and gun design requirements for an X-band MBK [5,9].

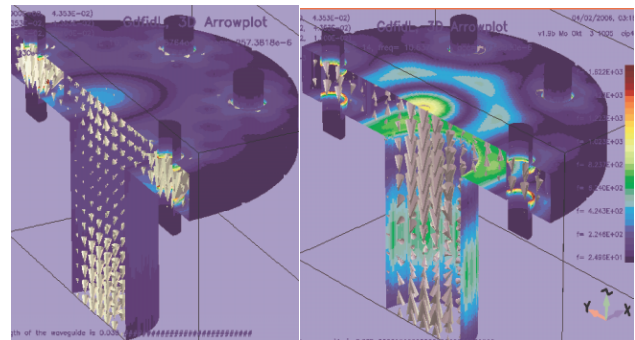


Figure 6: Six-beam TM_{020} (on the left) and TM_{030} (on the right) modes for a PBG cavity with $a/b=0.066$ coupled with a central TM_{01} circular pipe.

The external Q-factor is calculated with three methods: frequency detuning with a movable short-cut termination [10,11], idealized absorber (both with 3D eigenmode solver), and with discrete source and absorber (in a time-domain). The first method gives the best accuracy. The minimal external Q-factors obtained are 10 for TM_{030} mode and 79 for TM_{020} (see Figure 6). These are well below the Q-factors we estimated for the MBK taking into account the $R/Q (<25\Omega)$ per beamlet used in the 1D klystron simulation [13]. Although the low R/Q facilitates the outcoupler design, efficiency issues may require multi-cavity outcoupling. This can be done by stacking several cavities sharing the same central pipe.

We also studied field uniformity between adjacent beam-cavity interaction sites with both 2D and 3D codes. For the worst case when a close parasitic quadrupole mode can affect the operating mode, we have 1.6% difference in the R/Q , using a very fine ($43\mu m$) 3D

hexahedral mesh at 11.4 GHz frequency. Similar result is obtained with 2D triangular mesh calculation.

Another issue is frequency separation $\Delta f/f$. Numerous runs of different 6-beamlet configurations with or without rods indicate that the frequency “gap” between two parasitic modes with the TM_{0N0} operating mode in-between does not exceed 10-12%. With 6×8 rods, we found a value of $\Delta f/f = 5\%$ between the TM_{030} mode and the closest parasitic mode (quadrupole for reentrant cavity shape). While the R/Q for the TM_{020} mode is more than twice as large, the frequency separation and field uniformity (~1-2%) are not as good.

One can reduce the number of rods down to 6×6 as shown in Figure 7. For this configuration, the TM_{030} operating mode gives $R/Q=6.7\Omega$ and $\Delta f/f = 4.5\%$.

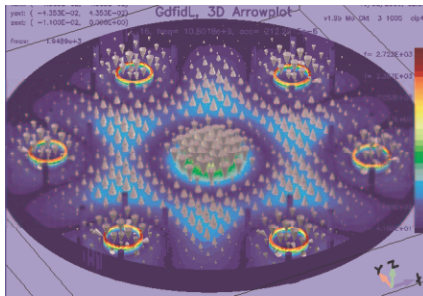


Figure 7: 6-beam TM_{030} cavity with 36 rods.

TWO-BEAM FLAT-FIELD CAVITY

We introduced earlier [12] a single sheet-beam, flat-field cavity having at least two rows of rods to provide field flatness. Other features of this cavity include a large vacuum conductivity with room for diagnostics or laser beam instrumentation (*e.g.* for lasertron). However, if the beam is too wide, the frequency separation can become quite small. A possible improvement is to have two beams instead of one. For a high-power klystron with a high total perveance it is also better to have more than just a single beam for reduced space charge effect. For example, the SLAC SBK configuration [13] foresees two sheet beams. Figure 8 presents a GdfidL design of a two-sheet-beam cavity. It is a rectangular cavity loaded with just a single row of rods.

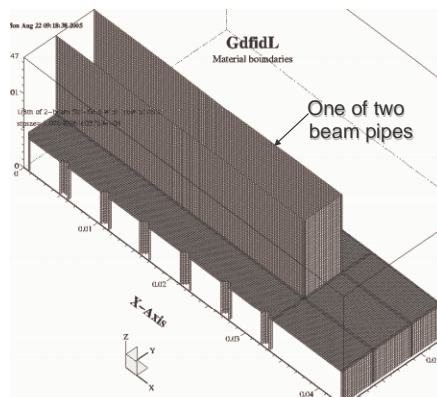


Figure 8: One eighth of a two-sheet-beam cavity having only one row of 13 rods.

Good field flatness (see Figure 9) can be achieved with just a wall in place of the rods. However, the rods provide the “transparency” feature and can be used also for fine adjustment of the flatness including their non-equidistant placement.

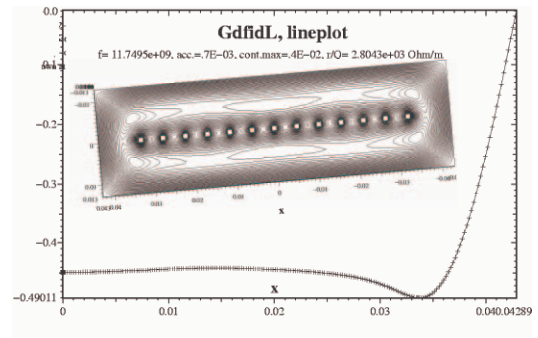


Figure 9: Linear and contour plots of the longitudinal electric field for the operating mode in a two-sheet-beam rod-loaded cavity.

ACKNOWLEDGEMENTS

We are grateful to Richard Temkin and (late) Norman Kroll for their encouragement. We appreciate Ping Chen for the postprocessor provided for SUPERFISH.

REFERENCES

- [1] M.A. Shapiro, J.R. Sirigiri, R.J. Temkin, G. Shvets in Proc. of the PAC 2005 Conf. (2005) 1838
- [2] N. Kroll, D. Smith, S. Shultz, Advanced Accelerator Concepts Workshop, Port Jefferson, New York, AIP Conf. Proc., v. 279, AIP 279 (1992) 197.
- [3] W. Bruns: GdfidL v. 1.8: Syntax and Semantics. (2002)
- [4] J.H. Billen, L.M. Young, Poisson Superfish codes, v. 7.14, Los Alamos
- [5] A. V. Smirnov, D. Yu, in Proc. of the PAC 2005 Conf. (2005) 3094
- [6] A.V. Smirnov, D. Yu, in AIP Conf. Proc., v. 737 (2004) 722.
- [7] W. Bruns: GdfidL.02: Syntax, Institut für Theoretische Elektrotechnik Technische Universität Berlin (1998)
- [8] L. Derun, N. Kroll, S. Schultz, in Proc. of Workshop on Advanced Accelerator Concepts, AIP Conf. Proc., v. 398, Lake Tahoe, CA (1996) 528
- [9] DOE SBIR Phase II Final Report. Grant # DE – FG03-93ER81573, DULY Research Inc. (1997).
- [10] J.C. Slater, *Microwave Electronics*, D. Van Nostrand Co. Inc, Princeton, NJ. 1959.
- [11] N. Kroll and D. Yu, *Particle Accelerators*, V. 34 (1990) 231.
- [12] D. Yu, D. Newsham, A. Smirnov, Proceedings of PAC03, p. 1153.
- [13] G. Caryotakis. SLAC Klystron Lectures, http://www-group.slac.stanford.edu/kly/Old_web_site/slac_klystron_lecture_series.htm